Hindawi
Advances in Materials Science and Engineering
Volume 2022, Article ID 8114708, 6 pages
https://doi.org/10.1155/2022/8114708

Research Article

Analysis of the Pile-Soil Combined Effect of Micropiles in Strengthening Expansive Soil Landslide in Southern Shaanxi Based on the Dynamic Soil Arch Model

Xiao Ding,[1,2] **Hui He**,[1,2] **Yonglong Qu**,[1,2] **and Yixuan Yang**[1,2]

[1]*School of Civil and Architecture Engineering, Xi'an Technological University, Xi'an, Shannxi 710021, China*
[2]*Xi'an Key Laboratory of Civil Engineering Testing and Destruction Analysis on Military-Civil Dual Use Technology, Xi'an, China*

Correspondence should be addressed to Xiao Ding; dx_0402@163.com

Received 15 June 2022; Revised 7 November 2022; Accepted 8 November 2022; Published 14 November 2022

Academic Editor: Abhinay Kumar

Southern Shaanxi region is mountainous and landslide disasters are frequent. Micropile reinforcement technology is widely used in landslide management, especially in landslide emergency rescue projects, due to easy construction, small soil disturbance, and strong site adaptability. Soil arch effect is an important prerequisite for safe and economic performance of the support function of micropile. For the swelling soil landslide of the accumulation layer in southern Shaanxi, firstly, a numerical model is established by means of thermal-mechanical coupling of FLAC^{3D} to explore the variation of the soil arch form with different swelling forces. Then, two theoretical models are proposed under normal working condition and rainfall working condition. The evolution and failure mode of soil arch are analyzed. The results show that the soil expansion after rainfall causes the change of the soil arch mode, the range of pile-soil interaction is obviously reduced, and the soil arch effect is weakened. It should be considered in the design of micropiles in strengthening expansive soil landslide.

1. Introduction

The mountainous area of southern Shaanxi is located in the Qinling-Bashan mountains of China, with a complex geological structure and special climate. It is one of the areas with high incidence of geological disasters and serious disasters. Based on the investigation data of 3442 landslide disasters in the area, it is found that the accumulated layer landslide accounts for about 92.3% of the total number of landslides, shallow layer landslide accounts for 51%, middle layer landslide accounts for 42%, deep layer landslide accounts for 7%, and some of the landslides are expansive in nature [1, 2].

Lizzi [3] proposed the use of micropiles to manage landslides. Since then, many scholars have studied the reinforcement mechanism and design method of micropiles [4–6]. Micropiles are widely used in landslide management in southern Shaanxi Province. When reinforcing landslides, they play a role similar to that of retaining walls, in addition to improving the shear strength of landslides. Due to its structural characteristics of small pile diameter and high density of pile placement, the soil arch structure is formed between piles and multiple rows of piles work together to form a core antislip body [7].

Since Terzaghi [8] proposed the soil arch effect, many scholars have studied the soil arch effect [9–11]. The joint action of pile-soil and soil arch effect between piles has also been fully verified [12–14]. The soil arch effect is a prerequisite for the discontinuous support structure to produce a continuous support effect. By making full use of the soil arch effect, the self-bearing capacity of the soil can be brought into play and the design parameters of mini-piles can be determined in a reasonable and economic way. Previous studies have shown that the soil arch has the processes of generation, development, and fracture with the landslide thrust increase, and different stages result in different arching mode [15]. Based on the existing research results, the soil arching effect of expansive soil is studied in this paper.

Based on a landslide management project in Mianxian County, southern Shaanxi Province, this paper studies the effect of soil expansion on the pile-soil interaction after rainfall by applying the thermodynamic module of FLAC^{3D} software to simulate soil humidification and expansion through thermal expansion. According to the results of numerical simulation, the shape and force form of the soil arch between piles are analyzed. Then, two soil arch calculation models are proposed under normal working condition and rainfall working condition, the combined effect range of pile and soil is deduced, and the evolution process of the soil arch behind and between micropiles in strengthening expansive soil landslide is studied.

2. Numerical Simulation Analysis

2.1. Project Overview and Design Parameters of Micropile. A landslide in the north of Yangjiawan Village, Xinjiezi Town, Mianxian County, Hanzhong, is located on the southern edge of the mountain, with a gentler overall form at the front and steeper at the back edge, and the soil is medium-weak expansive soil. The landslide was numerically simulated with a model size of 100 m × 33.6 m × 40 m. Three rows of micropiles were used to reinforce the slope. The micropiles were arranged in plum shape, with a hole depth of 12 m, a hole diameter of 200 mm, a pile spacing of 1.6 m, a row spacing of 1.0 m, and an anchorage depth of 4 m. The landslide soil body adopted the Mohr–Coulomb model, and the pile-soil contact surface adopted the Coulomb shear intrinsic model. The simulation parameters are shown in Table 1.

2.2. Determination of Thermal Expansion Coefficient. WZ-2 swelling instrument was used for the unloaded swelling rate test, and the swelling force of the specimen was measured by triplex medium and low pressure consolidation instrument according to the load balance method. According to the test results, the swelling force of the specimen with moisture content of 18% and dry density of 1.5 was 9.91 kPa and the swelling amount was 1.725 mm [16]. The existing research results show that the temperature field can be used to simulate the humidity field [17]. The ring knife model of the swelling soil was established. Through the thermodynamic module of FLAC^{3D}, the thermal-force coupling analysis was carried out to monitor the stress and displacement on the upper surface of the ring knife model and invert the thermal expansion coefficient of the soil, as shown in Table 2. To study the effect of soil swelling on the combined effect of pile and soil, different swelling forces can be obtained by varying the swelling coefficients, as shown in Table 3.

2.3. Effects of Soil Expansion on the Combined Effect of Pile and Soil. The simulated swelling forces in the soil are 0 kPa, 9.92 kPa, 15.06 kPa, and 19.96 kPa, and the stresses in the y-direction are shown in Figure 1.

The simulation results show that when there is no swelling force, the first row of interpile soil arches are fully developed, and an obvious triangular stress superposition zone is formed in front of the pile, which indicates the formation of soil arches at the pile ends. When the swelling force increases to 9.92 kPa, the soil between the piles is squeezed towards the two piles due to the swelling force, the frictional resistance on the pile-soil interface increases, a butterfly-shaped stress area is formed in two sides of the pile, and the soil arch sag between the piles decreases, the combined effect range between the pile and soil becomes smaller. The soil arch at the pile end is transformed into the friction soil arch at the pile side. When the swelling force continues to increase to 15.06 kPa, only residual strength remains in the soil between the first row of piles, the combined effect of the pile and soil fails, the soil between the piles flows, and the landslide thrust is transferred to the second row of piles. When the swelling force is 19.96 kPa, the soil between the first row of piles loses its antislip ability, the arch in the second row of piles degrades to pillow shape, and the landslide thrust is transferred to the soil of the third row of piles.

3. Calculation of the Soil Arch Effect between Piles

3.1. Analysis of the Combined Effect of Pile-Soil under Normal Working Conditions. The soil arch form at the pile end is analyzed by a three-hinged arch, whose axis is a reasonable arch axis, and there is only axial force but no shear force and bending moment on the arch cross section. As shown in Figure 2, due to the symmetry of the arch structure, half arch is taken for analysis, q is the landslide thrust, l is the soil arch span, f is the soil arch vector height, t is the soil arch thickness, and F_{Ax} and F_{Ay} are the horizontal and vertical support reactions at the arch foot.

According to the vertical static equilibrium condition $F_{Ay} - 1/2ql = 0$, it is obtained as follows:

$$F_{Ay} = \frac{ql}{2}. \tag{1}$$

For the moment of point C at the top, there is

$$F_{Ax} f - F_{Ay} \frac{l}{2} + \frac{ql^2}{4} = 0. \tag{2}$$

The horizontal direction support reaction force can be obtained as follows:

$$F_{Ax} = \frac{ql^2}{8f}. \tag{3}$$

Substitute equations (1) and (3) into equation (2) to obtain the arch axis equation:

$$y = \frac{4fx(l-x)}{l^2}. \tag{4}$$

The axial force at the arch foot on the arch axis is as follows:

$$N = \sqrt{{F_{Ax}}^2 + {F_{Ay}}^2} = \frac{ql\sqrt{l^2 + 16f^2}}{8f}. \tag{5}$$

High span relationship is as follows:

Table 1: Numerical simulation mechanical parameters.

Name	Elastic modulus (Pa)	Poisson's ratio	Cohesive force (kPa)	Internal friction angle (°)
Sliding mass	2×10^{7}	0.3	50	21.3
Landslide bed	1.8×10^{9}	0.2	70	30
Micropiles	2.5×10^{10}	0.15	—	—

Table 2: Inversion of thermal expansion coefficient of expansive soil.

Thermal expansion coefficient (1/°C)	Simulated swelling force (kPa)	Tested swelling force (kPa)	Swelling force error (%)	Simulated swelling amount (mm)	Tested swelling amount (mm)	Swelling amount error (%)
8.51×10^{-4}	9.92	9.91	0.1	1.758	1.725	1.9

Table 3: Relationship between thermal expansion coefficient and swelling force in software.

Thermal expansion coefficient (1/°C)	Swelling force (kPa)
0	0
8.51×10^{-4}	9.92
1.29×10^{-3}	15.06
1.71×10^{-3}	19.96

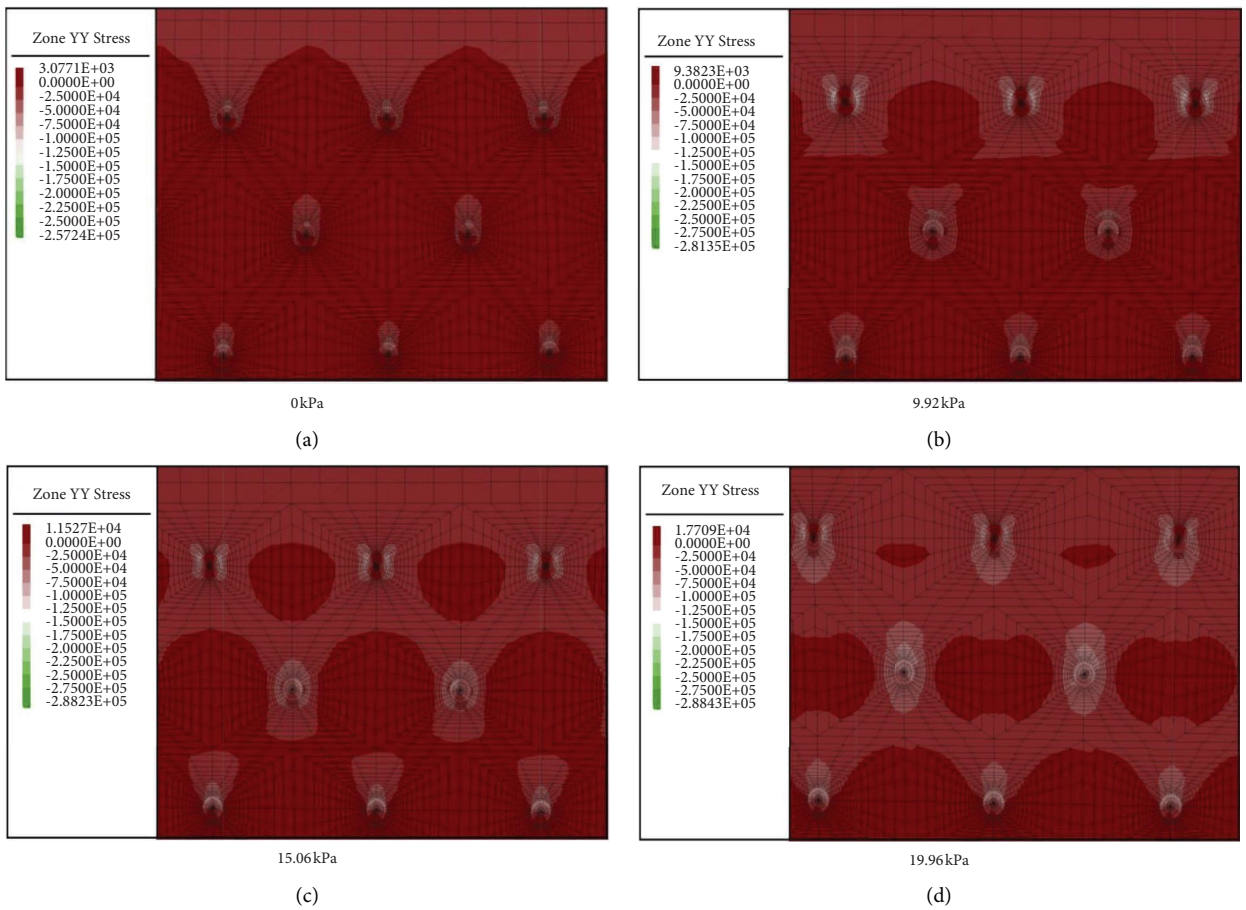

Figure 1: Positive stress in y-direction under different swelling forces. (a) 0 kPa, (b) 9.92 kPa, (c) 15.06 kPa, and (d) 19.96 kPa.

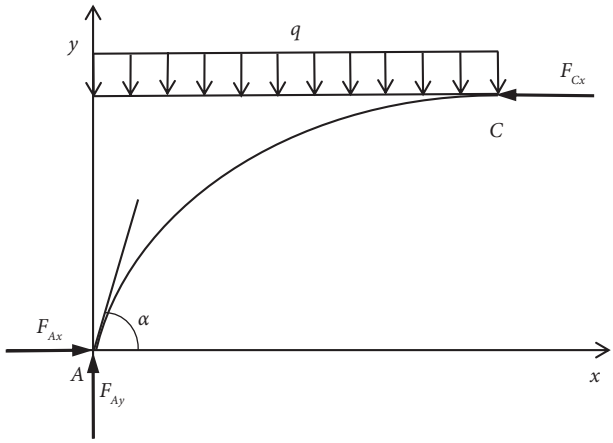

Figure 2: The force analysis of the soil arch between piles.

$$\tan\alpha = \frac{4f}{l}. \tag{6}$$

Force analysis of the triangular pressure zone at the arch foot is shown in Figure 3. The failure mode of the soil arch at the pile end is as follows: shear failure occurs in the triangular pressure zone, and its failure surface is at δ angle with the surface of large main stress action, as shown in Figure 4.

According to equation (5), the compressive stress σ_0 at the arch foot is as follows:

$$\sigma_0 = \frac{N}{d\sin\theta} = \frac{ql\sqrt{l^2+16f^2}}{8fd\sin\theta} = \frac{ql}{2d\sin\theta\sin\alpha}. \tag{7}$$

According to the geometric relationship in Figure 3:

$$\theta = \frac{135^\circ}{2} + \frac{\phi}{4}. \tag{8}$$

It can be seen from Figure 4 that the stress state at the arch foot is

$$\begin{cases} \sigma_1 = 2\sigma_0\sin\alpha, \\ \sigma_3 = \sigma_0\cos\alpha. \end{cases} \tag{9}$$

Substitute equation (7) into equation (9), and it is obtained that:

$$\begin{cases} \sigma_1 = \dfrac{ql}{d\sin\theta}, \\ \sigma_3 = \dfrac{ql\cos\alpha}{2d\sin\alpha\sin\theta}. \end{cases} \tag{10}$$

Based on the Mohr–Coulomb criterion, there is

$$\sigma_1 = \sigma_3\tan^2\delta + 2c\tan\delta, \tag{11}$$

where $\delta = 45^\circ + \phi/2$.

Substitute equations (6) and (10) into equation (11), and the vector height of the soil arch can be obtained, that is, the influence range of the combined effect of piles and soil:

$$ql^2\tan\delta - 8fql + 16fcd\sin\theta\cdot\tan\delta = 0, \tag{12}$$

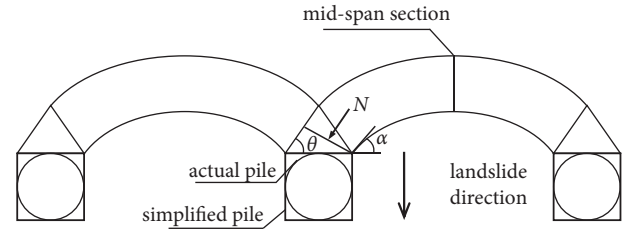

Figure 3: Force analysis of the triangular pressure zone at the arch foot.

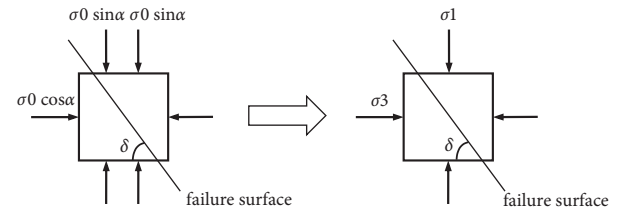

Figure 4: Stress distribution of microunits in the triangular pressure zone.

where q is the landslide thrust; l is the soil arch span; δ is the angle between the large principal stress surface and the failure surface; c is the soil cohesion; d is the pile diameter; f is the vector height of the soil arch.

3.2. Analysis of the Combined Effect of Pile and Soil When the Soil Swells under Rainfall Conditions. Under the rainfall condition, the swelling soil slope body expands and the soil arch between the piles fails in the span under the swelling force. Since it is assumed that the soil arch structure is a reasonable arch axis and the span center is a unidirectional force, the reason for the failure of the soil arch due to expansion is analyzed by the schematic diagram of the main stress change before and after the expansion of the microunit body, and the relationship between the Mohr circle and shear strength wrap is shown in Figures 5 and 6. The right circle in Figure 5 is a one-way compressive Mohr stress circle without considering the effect of swelling force, and the maximum principal stress it can bear is σ_1. When the soil is subjected to swelling stress, the large principal stress moves to the left and becomes $\sigma_1 + \sigma_p$, where σ_p is the swelling stress. The stress circle translates to the left, the stress circle cuts with the strength envelope, the soil is damaged, sheds backward, and squeezes the soil behind the arch. After the rear soil is extruded, the shear strength of the soil increases and the strength line moves up to reach a new equilibrium.

According to the relationship in the figure, it can be deduced that

$$\sigma_c = \sigma_p\tan^2\delta + 2c\tan\delta, \tag{13}$$

where σ_c is the major principal stress; σ_p is the swelling stress.

The failure mode of the pile-side friction soil arch: the midspan section is damaged, and the force on the midspan section is shown in Figure 7. It can be obtained as follows:

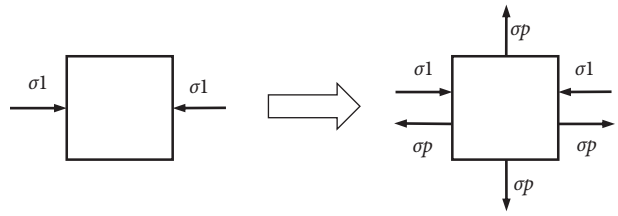

Figure 5: The main stress change before and after the expansion of the microunit body.

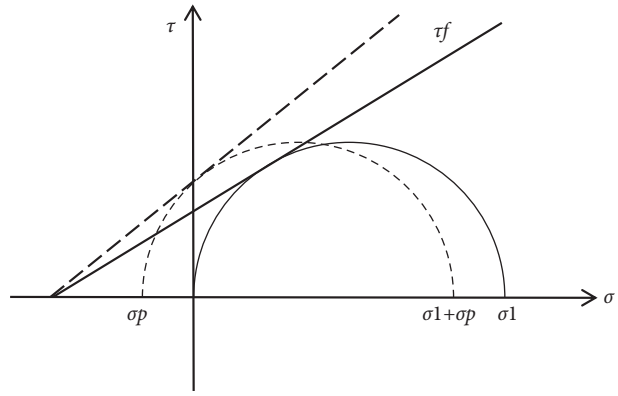

Figure 6: The relationship between the Mohr circle and shear strength wrap.

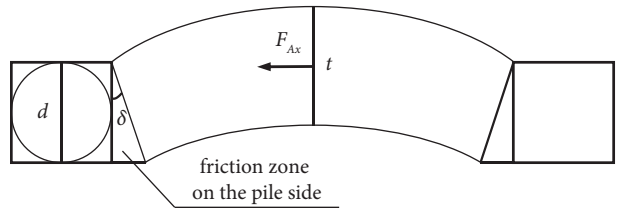

Figure 7: Schematic diagram of the force of the midspan section under the action of swelling force.

Table 4: Comparison between theoretical and simulated values of the combined effect range of pile and soil.

Calculation method	Influence range of pile front under normal working condition	Influence range of pile front under rainfall condition
Numeral calculation	0.4~0.6 m	0.2~0.3 m
Theoretical calculation	0.477 m	0.243 m

$$\sigma_c = \frac{F_{Ax}}{t} = \frac{ql^2 \cos\delta}{8 f d}. \tag{14}$$

Combining equations (13) and (14), it can be obtained as follows:

$$f = \frac{ql^2 \cos\delta}{8d\left(\sigma_p \tan^2\delta + 2c\tan\delta\right)}. \tag{15}$$

3.3. Comparison of Theoretical and Simulated Values of Engineering Examples. The example parameters are analyzed with the numerical simulation. The soil cohesion $c = 50$ kPa, internal friction angle $\varphi = 21.3^\circ$, landslide thrust $q = 45$ kPa, pile spacing $l = 1.6$ m, and pile diameter $d = 0.2$ m. When they are substituted into equation (12), the influence range of pile front under normal working condition can be obtained, which is similar to [15, 18]. When they are substituted into equation (15), the influence range of pile front can be obtained under rainfall condition when the swelling expansion force is $\sigma_p = 9.92$ kPa. The results are compared with the numerical simulation results in Table 4, and the theoretical calculation results are similar to the numerical calculation results.

4. Conclusion

(1) The landslide management project in Mianxian County is analyzed by applying the thermodynamic module of FLAC^{3D} software to simulate the humidity field through temperature field. Inverting the thermal expansion coefficients from the test data, the joint action of pile-soil and soil arch effect under different expansion forces can be simulated, and the

processes of soil arch generation, development, and fracture can be well presented.

(2) Considering the effect of soil expansion on the soil arch effect, according to the simulation results, it is concluded that the form of soil arch under normal working condition is the soil arch at the pile end. Under the rainfall condition, the expansion force changes the stress mode of pile-soil and the soil arch translates to the frictional soil arch on the pile side.

(3) The soil arch analysis model is established according to the soil arch failure model. Under normal working conditions, the compression zone of the arch triangle is damaged. Under rainfall conditions, the midspan section of the soil arch is damaged. The combined effect range of piles and soil under the two soil arching modes is deduced. Under normal working conditions, the combined effect range of pile and soil is 2~3 times the pile diameter, and the combined effect range of pile and soil after rainfall is 1~1.5 times the pile diameter. The results show that the soil expansion after rainfall causes the range reduction of pile-soil interaction and weakening of the soil arch effect.

Data Availability

The data used to support the findings of this study are included within the article.

Conflicts of Interest

The authors declare that there are no conflicts of interest regarding the publication of this paper.

Acknowledgments

The authors are grateful to the Science and Technology Planning Project of Shaanxi Province (2022JQ-443), Shaanxi Provincial Department of Education service local special project (22JC040), and scientific research program funded by Shaanxi Provincial Education Department (22JK0416) for the financial support.

References

[1] J. Wang, G. Yang, E. Hou, Z. Zhao, and H. Hui, *Research on Key Technology of Landslide Disaster Prevention in Southern Shaanxi Mountainous Area*, p. 20, Shaanxi Science and Technology Press, Xi 'an, 2015.

[2] H. Hui, *Research on micropile reinforcing mechanism and application of expansive soil landslides in shallow accumulative layer*, [Ph.D. thesis], p. 1, Xi'an University of Science and Technology, Xi 'an, 2013.

[3] F. Lizzi, *Reticulated Root Piles to Correct Landslides*, ASCE Convention and Exposition, Chicago, 1978.

[4] R. Cantoni, T. Collotta, and V. N. Ghionna, "A design method for reticulated micropiles structure in sliding slope," *Ground Engineering*, vol. 22, no. 1, pp. 41–47, 1989.

[5] H. Juran, A. Benslimane, and D. A. Bruce, *Slope Stabilization by Micropile Reinforcement*, pp. 1718–1726, Landslides, Kyoto, Japan, 1996.

[6] S. W. Sun, B. Z. Zhu, and J. C. Wang, "Design method for stabilization of earth slopes with micropiles," *Soils and Foundations*, vol. 53, no. 4, pp. 487–497, 2013.

[7] D. Mujah, H. Hazarika, N. Watanabe, and F. Ahmad, "Soil arching effect in sand reinforced with micropiles under lateral load," *Soil Mechanics and Foundation Engineering*, vol. 53, no. 3, pp. 152–157, 2016.

[8] K. Terzaghi, "The shearing resistance of saturated soils and the angle between the planes of shear," in *Proceedings of the 1st. International Conference on Soil Mechanics and Foundation Engineering*, Toronto, June 1936.

[9] R. Rui, A. F. van Tol, Y. Y. Xia, S. J. M. van Eekelen, and G. Hu, "Investigation of soilarching development in dense sand by 2D model tests," *Geotechnical Testing Journal*, vol. 39, no. 3, Article ID 20150130, 415 pages, , 2016.

[10] M. Al-Naddaf, J. Han, C. Xu, S. Jawad, and G. Abdulrasool, "Experimental investigation of soil arching mobilization and degradation under localized surface loading," *Journal of Geotechnical and Geoenvironmental Engineering*, vol. 145, no. 12, Article ID 04019114, 2019.

[11] L. Zhang, J. Zhou, S. Zhou, and Z. Xu, "Numerical spring-based trapdoor test on soil arching in pile-supported embankment," *Computers and Geotechnics*, vol. 148, p. 104765, Article ID 104765, 2022.

[12] R. Liang and S. Zeng, "Numerical study of soil arching mechanism in drilled shafts for slope stabilization," *Soils and Foundations*, vol. 42, no. 2, pp. 83–92, 2002.

[13] M. Ashour and H. Ar Da Lan, "Analysis of pile stabilized slopes based on soil-pile interaction," *Computers and Geotechnics*, vol. 39, no. 1, pp. 85–97, 2012.

[14] X. Hu, D. Liu, L. Niu, C. Liu, X. Wang, and R. Fu, "Development of soil-pile interactions and failure mechanisms in a pile-reinforced landslide," *Engineering Geology*, vol. 294, p. 106389, Article ID 106389, 2021.

[15] G. Chen, L. Zou, Q. Wang, and G. Zhang, "Pile-spacing calculation of anti-slide pile based on soil arching effect," *Advances in Civil Engineering*, vol. 2020, Article ID 7149379, 6 pages, 2020.

[16] Y. Yang, "Study on the mechanism of pile-soil interaction in strengthening expansive soil landslide of accumulation layer in southern shaanxi by miniature piles," pp. 34–40, Xi'an Technological University, Xi'an, 2020, [thesis].

[17] Z. Zeng, B. Xu, S. Hu, and C. Chen, "Numerical analysis of tunnel liner failure mechanism in expansive soil considering water-increased state," *Rock and Soil Mechanics*, vol. 35, no. 3, pp. 871–880, 2014.

[18] S. Gu and X. Zhen, "Analysis of micropile's slope reinforcement and determination of rational pile spacing," *Chinese Journal of Underground Space and Engineering*, vol. 11, no. 6, pp. 1617–1621, 2015.